

Digital Multi-Carrier Spread-Spectrum for Resistance against Jamming and Multipath

Shengli Zhou^{1*}, Georgios B. Giannakis^{1*} and Ananthram Swami²

¹ Dept. of ECE, Univ. of Minnesota, 200 Union Street SE, Minneapolis, MN 55455

² Army Research Lab, AMSRL-CI-CN, 2800 Powder Mill Rd, Adelphi, MD 20783

ABSTRACT

All-digital single-user Multi-Carrier Spread Spectrum (MC-SS) transceivers are studied in this paper and compared with Direct-Sequence Spread-Spectrum (DS-SS) systems under different scenarios. Closed-form bit error rate (BER) expressions are derived for sub-optimum matched filter and optimum minimum mean-square error reception in the presence of additive white Gaussian noise (AWGN) and Narrow-Band Interference (NBI). Although digital MC-SS turns out to outperform DS-SS, the difference is not as pronounced as in their analog counterparts. Closed-form BER expressions are also obtained for MC-SS and DS-SS transmissions propagating through frequency-selective multipath fading channels, and optimality is established for MC-SS when the channel taps are independent identically distributed (i.i.d.). But when the channel taps are non-i.i.d., MC-SS is shown to exhibit near-optimal behavior at high SNR and to outperform DS-SS even though their difference diminishes as the spreading factor increases and proper spreading codes are chosen for DS-SS. Finally, BER performance is carried out for MC-SS and DS-SS in the joint presence of multipath fading and NBI. Simulated BER evaluation illustrates the advantages of MC-SS over DS-SS in the presence of multipath and corroborates its robustness against AWGN and NBI.

1. INTRODUCTION

The increasing interest and applications of direct sequence spread spectrum (DS-SS) technology stem from its robustness to fading, its anti-interference capability, and the potential for (even uncoordinated) multiple access. An alternative to DS-SS signaling, called frequency-diversity spread spectrum (FD-SS), was recently proposed and shown to be more resistant than DS-SS to narrow band and partial band interference (NBI/PBI) [5]. FD-SS, with disjoint frequency support for each subcarrier, is, in fact, the analog counterpart of digital OFDM spread spectrum technique [9] and the underlying multicarrier spread spectrum (MC-SS) approach [12] for multicarrier (MC) CDMA with overlapping subcarriers. By exploiting multiple carriers and a narrow band DS waveform on each subcarrier, it has also been shown that multicarrier DS CDMA outperforms single carrier CDMA for wideband transmissions in the presence of narrow band interference [6].

Although most existing works rely on analog carrier modulations, digital implementations through FFTs are also available [5]. A unifying digital implementation framework of many existing schemes has been developed in [3, 11], which includes MC-CDMA [12] and MC-DS-CDMA [6] as special cases. Starting from a discrete-time equivalent model, we investigate the performance of digital MC-SS and compare it with DS-SS. The main contributions of this paper are the novel results on performance analysis of digital MC-SS in the presence of jamming and multipath. We focus on single user case in this paper.

The rest of this paper is organized as follows. The discrete-time system model is introduced in Section 2. MC-SS and DS-SS are then compared under various conditions: additive white Gaussian noise (AWGN) channels with narrow band and partial band interference (NBI/PBI) in Section 3, and frequency-selective multipath channels with NBI/PBI in Section 4. Conclusions are then drawn in Section 5.

2. DISCRETE-TIME SIGNAL MODEL

We adopt the unifying framework developed by Zhou *et al.*, [13], which describes both MC-SS and DS-SS systems; see Fig. 1 which depicts the discrete-time baseband equivalent models.

In MC-SS, the length- N symbol periodic digital spreading code \mathbf{c}_{mc} spreads the i th information symbol $s(i)$. The length N IFFT of the resulting $N \times 1$ vector $\mathbf{c}_{mc}s(i)$ is computed, and a cyclic prefix (CP) inserted to yield the $P \times 1$ vector, $\mathbf{u}(i)$. To avoid inter-block interference (IBI), we must have $P \geq N + L$, where L is the channel order. To avoid bandwidth overexpansion, we choose the smallest block length:

As0): The transmitted block length $P = N + L$.

* Supported by ARL grant no. DAAL01-98-Q-0648 and NSF Wireless Initiative grant no. 99-79443.

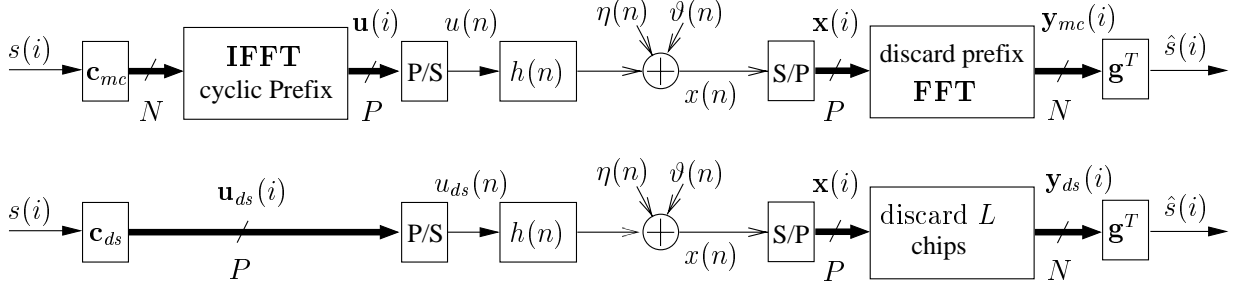


Figure 1. Discrete-time equivalent baseband model for MC-SS (upper part) and DS-SS (lower part)

In the presence of additive Gaussian noise (AGN) $\eta_c(t)$ and NBI $\vartheta_c(t)$, the received signal, sampled at the chip rate, is

$$x(n) = h(n) \star u(n) + \eta(n) + \vartheta(n) = \sum_{l=0}^L h(l)u(n-l) + \eta(n) + \vartheta(n), \quad (1)$$

where $\eta(n)$ and $\vartheta(n)$ are filtered AGN and NBI, respectively. Because the pulse shaper has Nyquist characteristics by design, $\eta(n)$ is white if $\eta_c(t)$ is.

Notation (see details in [13]): Define $\mathbf{h} := [h(0), \dots, h(L)]^T$, and $\bar{\mathbf{w}}(i)$ to be the composite noise and interference vector. Let $\mathbf{D}(\mathbf{c}) := \text{diag}(\mathbf{c})$ denote a diagonal matrix whose diagonal is the vector \mathbf{c} ; \mathbf{F}_N the $N \times N$ FFT matrix, \mathbf{V} the $N \times (L+1)$ Vandermonde matrix formed by the first $L+1$ columns of $\sqrt{N}\mathbf{F}_N$, and let \mathbf{C}_{ds} denote the $N \times (L+1)$ Toeplitz matrix with first column $[c_{ds}(L), \dots, c_{ds}(P-1)]$, and first row $[c_{ds}(L), \dots, c_{ds}(0)]$.

Next, we quote results from [13]. A unifying model is given by

$$\mathbf{y}(i) = \mathbf{C}\mathbf{h}s(i) + \mathbf{w}(i) = \mathbf{c}s(i) + \mathbf{w}(i), \quad (2)$$

where \mathbf{c} denotes the equivalent signature code vector after channel convolution and receiver processing. For convenience, we list the corresponding vectors for MC-SS and DS-SS unified by (2):

$$\mathbf{y}(i) = \mathbf{D}^{\mathcal{H}}(\mathbf{c}_{mc})\mathbf{y}_{mc}(i), \quad \mathbf{c} = \mathbf{V}\mathbf{h}, \quad \mathbf{w}(i) = \mathbf{D}^{\mathcal{H}}(\mathbf{c}_{mc})\mathbf{F}_N\bar{\mathbf{w}}(i), \quad \text{for MC-SS}, \quad (3)$$

$$\mathbf{y}(i) = \mathbf{y}_{ds}(i), \quad \mathbf{c} = \mathbf{C}_{ds}\mathbf{h}, \quad \mathbf{w}(i) = \bar{\mathbf{w}}(i), \quad \text{for DS-SS}. \quad (4)$$

The corresponding SNR at the output of the matched filter (MF), $\mathbf{g}_{mf}^T := \mathbf{c}^{\mathcal{H}}$, is thus:

$$SNR_{mf} = \frac{|\mathbf{g}_{mf}^T \mathbf{c}s|^2}{\mathbb{E} \left\{ |\mathbf{g}_{mf}^T \mathbf{w}|^2 \right\}} = \frac{\sigma_s^2 |\mathbf{c}^{\mathcal{H}} \mathbf{c}|^2}{\mathbf{c}^{\mathcal{H}} \mathbf{R}_{ww} \mathbf{c}}, \quad (5)$$

where $\mathbf{R}_{ww} := \mathbb{E} \{ \mathbf{w}(i) \mathbf{w}^{\mathcal{H}}(i) \}$. The SNR at the output of the optimum minimum mean-square error (MMSE) receiver, $\mathbf{g}_{mmse}^T = \mathbf{c}^{\mathcal{H}} \mathbf{R}_{ww}^{-1}$, is given by

$$SNR_{mmse} := \frac{|\mathbf{g}_{mmse}^T \mathbf{c}s|^2}{\mathbb{E} \left\{ |\mathbf{g}_{mmse}^T \mathbf{w}|^2 \right\}} = \sigma_s^2 \mathbf{c}^{\mathcal{H}} \mathbf{R}_{ww}^{-1} \mathbf{c}. \quad (6)$$

3. AWGN CHANNEL WITH NARROW BAND INTERFERENCE

In this section, we focus on the ability of digital MC-SS and DS-SS to suppress narrow band interference. We will assume the channel is non-fading AWGN, i.e., $L = 0$, and $\mathbf{h} = h(0) = 1$. This case was also considered in [5] to compare DS-SS with FD-SS, which is the analog counterpart of the digital MC-SS that we developed in the previous section.

Due to the existence of NBI/PBI, the composite noise $\bar{\mathbf{w}}(i)$ is no longer white. We define its $N \times N$ correlation matrix as: $\mathbf{R}_{\bar{\mathbf{w}}} := \mathbb{E} \{ \bar{\mathbf{w}}(i) \bar{\mathbf{w}}^{\mathcal{H}}(i) \}$. Since the entries of $\bar{\mathbf{w}}(i)$ are samples from a stationary Gaussian process, we can approximate its

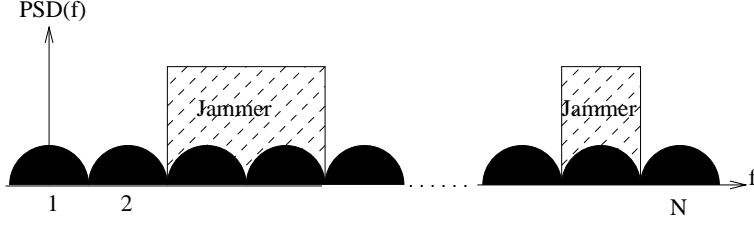


Figure 2. Signal and interference spectra: A simple example

correlation matrix by a circulant matrix when the size N is large. [1, pp. 73-74]. Therefore, we can approximately diagonalize the correlation matrix by (I)FFT matrices; we assume that the diagonalization is perfect:

As1) $\mathbf{F}_N \mathbf{R}_{\bar{w}\bar{w}} \mathbf{F}_N^H = \mathbf{\Delta}$, where $\mathbf{\Delta}$ is a diagonal matrix with positive diagonal entries $\delta_{11}, \dots, \delta_{NN}$.

Because the FFT is asymptotically equivalent to the Karhunen-Loève Transform (KLT), the entries of the FFT output $\mathbf{F}_N \bar{\mathbf{w}}(i)$ are asymptotically uncorrelated random variables [1]. Therefore, assumption As1) becomes more and more accurate as the FFT size N increases (i.e., the spreading code length increases). See Remark 1 for comments on the case where As1) does not hold exactly.

For illustrative purposes, we construct a simple example, where we assume that the jammer has the same power in every subband where it is present; see Fig. 2, and also [5, 6] for related examples. Thus, the $N \times N$ diagonal matrix $\mathbf{\Delta}$ in As1) has entries:

$$\delta_{ii} = \begin{cases} (J_0 + N_0)/2 & \text{when jammer is present in the } i\text{th subband} \\ N_0/2 & \text{when jammer is absent in the } i\text{th subband} \end{cases}, \quad (7)$$

where $N_0/2$ is the power spectrum density (PSD) of the additive white noise $\eta_c(t)$, and $J_0/2$ is the PSD of the narrow band jammer. Suppose that $\vartheta_c(t)$ occupies ϵB bandwidth ($0 < \epsilon < 1$) which implies that there are ϵN (we assume ϵN to be integer for simplicity) subbands hit by jammers. We can then rewrite $\mathbf{\Delta}$ as:

$$\mathbf{\Delta} = (N_0/2)\mathbf{I}_N + (J_0/2)\mathbf{I}'_N, \quad (8)$$

where \mathbf{I}'_N has ϵN unity entries on the diagonal (when NBI/PBI is present in those subbands) and all other entries are zero.

We now evaluate the SNR and Bit Error Rate (BER) for MC-SS and DS-SS; for simplicity, we assume BPSK modulation in this section.

3.1. MC-SS

Under As1), we obtain the noise correlation matrix for MC-SS as:

$$\mathbf{R}_{ww}^{(mc)} = \mathbf{D}^H(\mathbf{c}_{mc}) \mathbf{F}_N \mathbf{R}_{\bar{w}\bar{w}} \mathbf{F}_N^H \mathbf{D}(\mathbf{c}_{mc}) = \mathbf{\Delta}, \quad (9)$$

which follows since the spreading sequence \mathbf{c}_{mc} has ± 1 entries.

With $\mathbf{h} = h(0) = 1$, $\mathbf{c} = \mathbf{V}\mathbf{h} = \mathbf{1}_{N \times 1}$ ($\mathbf{1}_{N \times 1}$ denotes an $N \times 1$ vector with all unit entries) in (3), and $\mathbf{R}_{ww}^{(mc)}$ given by (9), we can simplify (5) and (6) for MC-SS as:

$$SNR_{mf}^{(mc)} = \frac{N^2 \sigma_s^2}{\text{tr}\{\mathbf{\Delta}\}}, \quad SNR_{mmse}^{(mc)} = \sigma_s^2 \text{tr}\{\mathbf{\Delta}^{-1}\}, \quad (10)$$

where $\text{tr}\{\cdot\}$ is the trace operator. Since the arithmetic mean cannot be smaller than the harmonic mean, we have $\text{tr}\{\mathbf{\Delta}^{-1}\} \geq N^2 / \text{tr}\{\mathbf{\Delta}\}$, so that $SNR_{mmse}^{(mc)} \geq SNR_{mf}^{(mc)}$, as expected. We infer that the MMSE receiver outperforms the MF receiver, which, of course, is suboptimal in the presence of colored noise.

In the special case of (8), we have $\text{tr}\{\mathbf{\Delta}\} = N(N_0/2 + \epsilon J_0/2)$ and $\text{tr}\{\mathbf{\Delta}^{-1}\} = N[2\epsilon/(J_0 + N_0) + 2(1 - \epsilon)/N_0]$, so that (10) becomes

$$SNR_{mf}^{(mc)} = \frac{2N\sigma_s^2}{N_0} \frac{1}{1 + \epsilon J_0/N_0}, \quad SNR_{mmse}^{(mc)} = \frac{2N\sigma_s^2}{N_0} \left(\frac{\epsilon}{1 + J_0/N_0} + 1 - \epsilon \right). \quad (11)$$

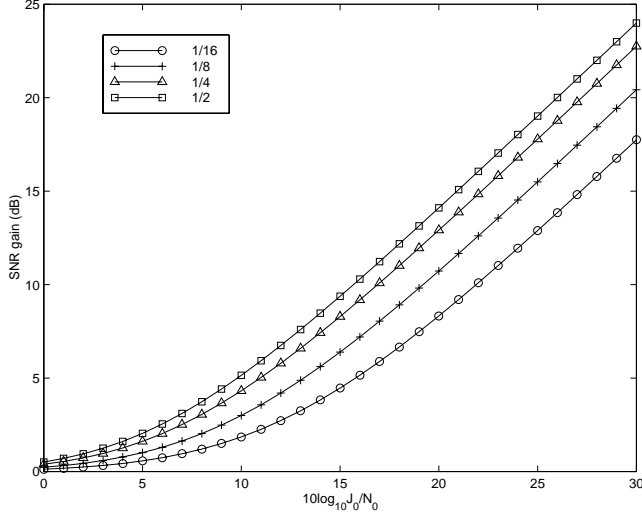


Figure 3. SNR gain of MMSE over MF receiver as a function of interference power to AWGN variance, with curves parameterized by ϵ , the fractional bandwidth of the interference.

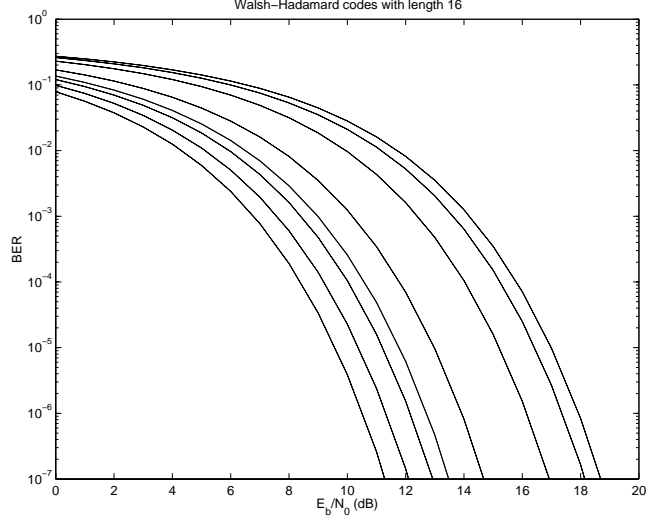


Figure 4. BER for DS-SS with different W-H codes.

Define the bit energy $E_b := N\sigma_s^2$, and parameters $\beta_{mf}^{(mc)} := 1/(1 + \epsilon J_0/N_0)$, and $\beta_{mmse}^{(mc)} = \epsilon/(1 + J_0/N_0) + 1 - \epsilon$. Based on (11), the corresponding closed-form BER expressions for BPSK can be found as [8, p. 258]:

$$P_{b,mf}^{(mc)} = Q\left(\sqrt{SNR_{mf}^{(mc)}}\right) = Q\left(\sqrt{\frac{2E_b}{N_0}\beta_{mf}^{(mc)}}\right), \quad (12)$$

$$P_{b,mmse}^{(mc)} = Q\left(\sqrt{SNR_{mmse}^{(mc)}}\right) = Q\left(\sqrt{\frac{2E_b}{N_0}\beta_{mmse}^{(mc)}}\right),$$

where $Q(\cdot)$ denotes the Q -function. Parameters $\beta_{mf}^{(mc)}$ and $\beta_{mmse}^{(mc)}$ are both less than unity and indicate the SNR loss for MC-SS relative to a transmission over an AWGN channel with $SNR = 2E_b/N_0$. In order to achieve the same error probability as in the unjammed AWGN case, bit energy E_b must be increased by a factor of $1/\beta_{mf}^{(mc)}$ or $1/\beta_{mmse}^{(mc)}$.

As J_0/N_0 increases, both $\beta_{mf}^{(mc)}$ and $\beta_{mmse}^{(mc)}$ decrease and consequently the BER performance degrades as confirmed by (12). However, we notice that the SNR degradation is unbounded for the MF receiver, but is upper bounded for the MMSE receiver even when $J_0/N_0 \rightarrow \infty$, since the power degradation $1/\beta_{mmse}^{(mc)} \leq 1/(1 - \epsilon)$. To compare these two different receivers more clearly, we define the SNR gain of the MMSE over the MF receiver as:

$$\mathcal{G} := \beta_{mmse}^{(mc)} / \beta_{mf}^{(mc)} = 1 + \epsilon(1 - \epsilon) \frac{(J_0/N_0)^2}{1 + (J_0/N_0)}. \quad (13)$$

From (13), we find that $\beta_{mmse}^{(mc)} \geq \beta_{mf}^{(mc)}$, with equality at $\epsilon = 0$ (no NBI) or $\epsilon = 1$ (NBI occupies the full band); both of these cases correspond to white noise. In Fig. 3, we plot the SNR gain in (13) versus power density ratio J_0/N_0 , for different values of the NBI parameter $\epsilon = [1/16, 1/8, 1/4, 1/2]$. Even for a moderate power NBI, say with $\epsilon = 1/16$, and $J_0/N_0 = 15$ dB, the gain is 5 dB, and increases with ϵ and J_0/N_0 . In the presence of colored noise, the optimum MMSE receiver significantly outperforms the suboptimum MF receiver, especially as the power spectrum density of NBI and the jammed bandwidth percentage increase. For a fixed J_0/N_0 , the SNR gain \mathcal{G} peaks at $\epsilon = 1/2$ which can be inferred from (13). Given a fixed average jamming power $J = \epsilon W_x J_0$ (W_x denotes the system bandwidth), it has been shown in [5] that the worst jammer for the MMSE receiver spreads its power evenly over the entire signal bandwidth, i.e., $\epsilon = 1$; in this case the MMSE receiver reduces to the conventional MF receiver and thus the SNR gain becomes $\mathcal{G} = 1$.

In this subsection, we showed that the MMSE receiver (which has knowledge of which subbands are jammed, and the jammer power to AWGN ratio) outperforms the MF receiver; the SNR gain of the MMSE receiver with respect to the MF

receiver, \mathcal{G} of (13), increases as the jammer power or the bandwidth occupied by the jammer increases. Further, a smart adversary spreads its power evenly, so that the MF (equivalent to MMSE now) is optimal. The SNR/BER performance is independent of the spreading code.

3.2. DS-SS

For DS-SS, we have $\mathbf{c} = \mathbf{C}\mathbf{h} = \bar{\mathbf{c}}_{ds} = \mathbf{c}_{ds}$ in (4) and $\mathbf{R}_{ww}^{(ds)} = \mathbf{R}_{\bar{w}\bar{w}} = \mathbf{F}_N^H \mathbf{\Delta} \mathbf{F}_N$ as per As1); the SNR in (5) and (6) can be simplified as

$$SNR_{mf}^{(ds)} = \frac{N^2 \sigma_s^2}{\mathbf{c}_{ds}^H \mathbf{F}_N^H \mathbf{\Delta} \mathbf{F}_N \mathbf{c}_{ds}}, \quad SNR_{mmse}^{(ds)} = \sigma_s^2 \mathbf{c}_{ds}^H \mathbf{F}_N^H \mathbf{\Delta}^{-1} \mathbf{F}_N \mathbf{c}_{ds}. \quad (14)$$

We see from (14) that the SNRs for DS-SS are *code dependent*, in contrast with the case for MC-SS in (10). Thus, the BER performance will be different for differently chosen spreading codes \mathbf{c}_{ds} . We illustrate this in Fig. 4 where the BER performance of the MF receiver for DS-SS, [c.f. (12)], is depicted for different Walsh-Hadamard (W-H) codes of length $P = 16$ in the presence of a jammer with spread $\epsilon = 3/16$, and jammer-to-noise ratio $10 \log_{10}(J_0/N_0) = 10\text{dB}$. Intuitively speaking, the spectrum of any particular code vector, \mathbf{c}_{ds} , is generally not flat, i.e., $\mathbf{F}_N \mathbf{c}_{ds}$ does not have all entries with unit amplitude, so that the result in (10) is not directly applicable. When the jammer hits the subband where the signal power is strong, the BER degradation becomes more pronounced.

To avoid the code dependence, we may adopt either code hopping (a scheme in which each user in a short code system switches among a predetermined set of code sequences [7]), or long code spreading, where the code period is much larger than the symbol period [7]. Let us suppose that there are N_c codes in a code hopping system with codes $\{\mathbf{c}_{ds,n}\}_{n=1}^{N_c}$. Let $SNR_{mf,n}^{(ds)}$ denote the output SNR resulting from the n th code, obtained by substituting \mathbf{c}_{ds} in (14) with $\mathbf{c}_{ds,n}$. For the MF receiver, the *average* SNR and BER are then given by

$$SNR_{mf}^{(ds)} = \frac{1}{N_c} \sum_{n=1}^{N_c} SNR_{mf,n}^{(ds)}, \quad P_{b,mf}^{(ds)} = \frac{1}{N_c} \sum_{n=1}^{N_c} \mathcal{Q} \left(\sqrt{SNR_{mf,n}^{(ds)}} \right). \quad (15)$$

For long code spreading, we assume that the code period is sufficiently long so that the chips can be thought of as being uncorrelated, i.e., $\mathbf{E} \{\mathbf{c}_{ds} \mathbf{c}_{ds}^H\} = \mathbf{I}_N$. Then, we have $\mathbf{E}_{\mathbf{c}_{ds}} \{\mathbf{c}_{ds}^H \mathbf{F}_N^H \mathbf{\Delta} \mathbf{F}_N \mathbf{c}_{ds}\} = \text{tr} \{\mathbf{E}_{\mathbf{c}_{ds}} \{\mathbf{c}_{ds} \mathbf{c}_{ds}^H \mathbf{F}_N^H \mathbf{\Delta} \mathbf{F}_N\}\} = \text{tr} \{\mathbf{\Delta}\}$, which results in an average SNR

$$\mathbf{E}_{\mathbf{c}_{ds}} \{SNR_{mf}^{(ds)}\} = \frac{N^2 \sigma_s^2}{\text{tr} \{\mathbf{\Delta}\}} = SNR_{mf}^{(mc)}. \quad (16)$$

Similarly, we have $\mathbf{E}_{\mathbf{c}_{ds}} \{\mathbf{c}_{ds}^H \mathbf{F}_N^H \mathbf{\Delta}^{-1} \mathbf{F}_N \mathbf{c}_{ds}\} = \text{tr} \{\mathbf{E}_{\mathbf{c}_{ds}} \{\mathbf{c}_{ds} \mathbf{c}_{ds}^H \mathbf{F}_N^H \mathbf{\Delta}^{-1} \mathbf{F}_N\}\} = \text{tr} \{\mathbf{\Delta}^{-1}\}$ and

$$\mathbf{E}_{\mathbf{c}_{ds}} \{SNR_{mmse}^{(ds)}\} = \sigma_s^2 \text{tr} \{\mathbf{\Delta}^{-1}\} = SNR_{mmse}^{(mc)}. \quad (17)$$

Although the average SNRs for long-code DS-SS coincides with those for MC-SS with symbol-periodic codes, the average BERs

$$P_{b,mf}^{(ds)} = \mathbf{E}_{\mathbf{c}_{ds}} \left\{ \mathcal{Q} \left(SNR_{mf}^{(ds)} \right) \right\}, \quad P_{b,mmse}^{(ds)} = \mathbf{E}_{\mathbf{c}_{ds}} \left\{ \mathcal{Q} \left(SNR_{mmse}^{(ds)} \right) \right\}, \quad (18)$$

may differ because $\mathbf{E}_{\mathbf{c}_{ds}} \left\{ \mathcal{Q} \left(SNR_{mf}^{(ds)} \right) \right\} \neq \mathcal{Q} \left(\mathbf{E}_{\mathbf{c}_{ds}} \left\{ SNR_{mf}^{(ds)} \right\} \right)$ in general. The latter implies that $P_{b,mf}^{(ds)} \neq P_{b,mf}^{(mc)}$, and similarly $P_{b,mmse}^{(ds)} \neq P_{b,mmse}^{(mc)}$. Note that the SNRs in (10) for MC-SS do not change with different \mathbf{c}_{mc} 's while the SNRs for DS-SS fluctuate around their means given by (16) and (17). Based on the fact that the average BER is dominated by worst cases, we may conclude that

$$P_{b,mf}^{(ds)} \geq P_{b,mf}^{(mc)}, \quad \text{and} \quad P_{b,mmse}^{(ds)} \geq P_{b,mmse}^{(mc)}. \quad (19)$$

However, the difference becomes small when the code period is sufficiently long. In Fig. 5(a), we plot the average BER [c.f. (15)] of a code hopping system with codes selected from the set of W-H codes of length 16. MC-SS has a 2dB advantage over DS-SS at BER of 10^{-6} if MF is used. In Fig. 5(b), the BER of a long code spreading DS-SS system [c.f. (18)] is depicted with period 1000 times the symbol period of $P = 16$ chips. In both cases, the jammer is the same as that leading to Fig. 4.

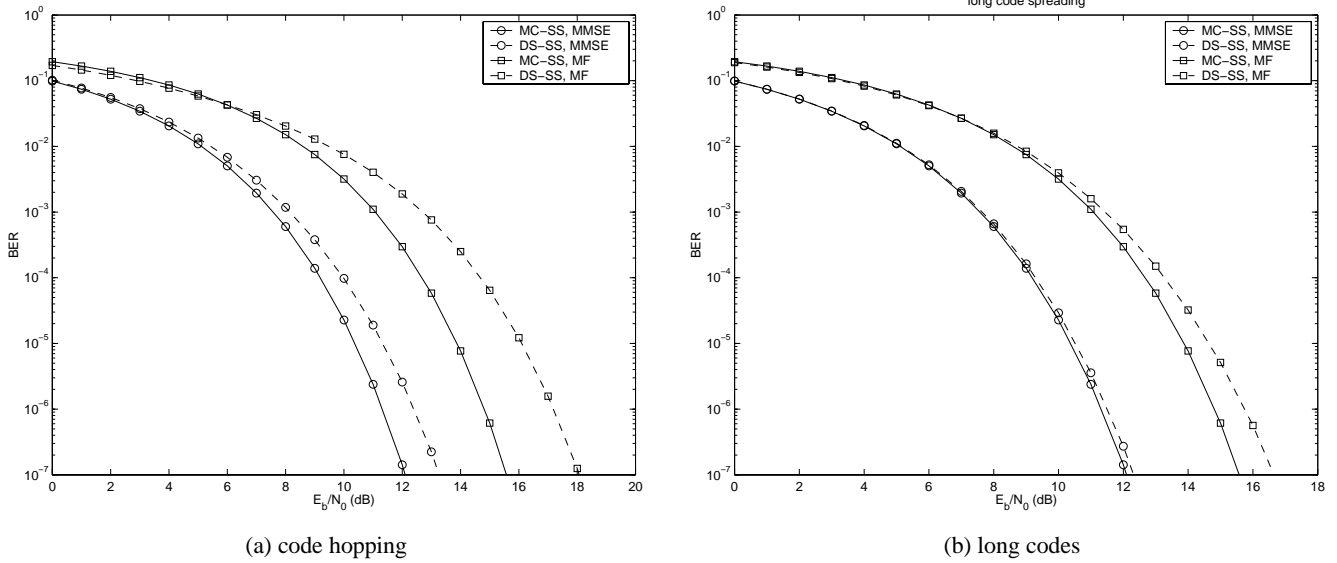


Figure 5. MC-SS versus DS-SS in the presence of AWGN and NBI/PBI

Comparing Fig. 5(a) with Fig. 5(b), we find that as the randomness of the code increases (code period increases), DS-SS performance approaches that of MC-SS.

Assuming long code spreading in DS-SS, the MF receiver and the average SNR expression of (16) were also derived in [5]. By tacitly assuming $E_{c_{ds}} \left\{ Q \left(SNR_{mf}^{(ds)} \right) \right\} = Q \left(E_{c_{ds}} \left\{ SNR_{mf}^{(ds)} \right\} \right)$ and thus $P_{b,mf}^{(ds)} = P_{b,mf}^{(mc)}$, it was asserted in [5] that

$$P_{b,mf}^{(ds)} \geq P_{b,mmse}^{(mc)}, \quad (20)$$

with the SNR gain of MC-SS over DS-SS equal to that given in (13).

The motivation behind adopting the MMSE receiver for FD-SS (MC-SS) and the MF receiver for DS-SS in [5] is implementation complexity. It turns out that the MMSE receiver is easy to build for analog MC-SS while it is difficult for DS-SS [5]. In contrast, with our digital transceivers, implementing MF or MMSE receivers for both MC-SS and DS-SS entails comparable complexity. Because the signal power is evenly distributed in each subband for MC-SS, it may be easier to detect the presence of jammers when the noise level is high. However, DS-SS can also improve its performance by MMSE reception after estimating the interference color by training or via blind adaptive algorithms. Although the conclusion that MC-SS is more robust to NBI than DS-SS has been reached for analog implementations in [5], where MC-SS and DS-SS employ different receivers. here, we see that the differences are much less pronounced.

Remark 1: If As1) does not hold exactly for MC-SS, we can express $\mathbf{F}_N \mathbf{R}_{\bar{w}\bar{w}} \mathbf{F}_N^H = \mathbf{\Delta} + \mathbf{E}$, where \mathbf{E} is a perturbation matrix having entries with small amplitudes. For MC-SS,

$$\mathbf{c}^H \mathbf{R}_{ww} \mathbf{c} = \mathbf{1}_{N \times 1} \mathbf{D}^H(\mathbf{c}_{mc}) \mathbf{F}_N \mathbf{R}_{\bar{w}\bar{w}} \mathbf{F}_N^H \mathbf{D}(\mathbf{c}_{mc}) \mathbf{1}_{N \times 1} = \mathbf{c}_{mc}^H \mathbf{F}_N \mathbf{R}_{\bar{w}\bar{w}} \mathbf{F}_N^H \mathbf{c}_{mc} = \text{tr} \{ \mathbf{\Delta} \} + \mathbf{c}_{mc}^H \mathbf{E} \mathbf{c}_{mc}.$$

Now, the SNRs in (5) and (6) for MC-SS also depend on the spreading code choice (in contrast with the case where $\mathbf{E} = 0$, leading to (10)). If we use code hopping or long code spreading, we can obtain the average SNRs following the same approach as that for the DS-SS:

$$E_{\mathbf{c}_{mc}} \left\{ SNR_{mf}^{(mc)} \right\} = \frac{N^2 \sigma_s^2}{\text{tr} \{ \mathbf{R}_{\bar{w}\bar{w}} \}} = E_{\mathbf{c}_{ds}} \left\{ SNR_{mf}^{(ds)} \right\}, \quad (21)$$

$$E_{\mathbf{c}_{mc}} \left\{ SNR_{mmse}^{(mc)} \right\} = \sigma_s^2 \text{tr} \{ \mathbf{R}_{\bar{w}\bar{w}}^{-1} \} = E_{\mathbf{c}_{ds}} \left\{ SNR_{mmse}^{(ds)} \right\}. \quad (22)$$

Although the average SNR is the same, we expect that the average BER is somewhat lower for MC-SS than for DS-SS, because the SNR for MC-SS has smaller fluctuations due to the fact that the perturbation matrix \mathbf{E} is negligible, i.e., As1) is basically satisfied.

In this subsection, we showed that the performance of DS-SS is code dependent; in order to eliminate this code dependency, one may want to hop among codes, or use long codes. In general, MC-SS outperforms DS-SS; the performance difference becomes less pronounced as the period of the (long) code increases. In analog implementations, MC-SS outperforms DS-SS considerably [5]; however, in digital implementations, and when MC-SS and DS-SS both use MF or both use MMSE receivers, the differences in performance become less pronounced. The performance of MC-SS also becomes code dependent if the noise is not white; code hopping is useful in this case. Recall that in this section, we assumed that the degradation is only due to AWGN and NBI/PBI.

4. MULTIPATH AND NBI/PBI

In this section, we consider the general case where NBI/PBI is present and the channel is frequency selective. Starting from the general model (2), we assume that \mathbf{c} and \mathbf{w} are random vectors with covariance matrices \mathbf{R}_{cc} and \mathbf{R}_{ww} , respectively. We then define

$$\mathbf{y}'(i) = \mathbf{R}_{ww}^{-1/2} \mathbf{y}(i) = \mathbf{R}_{ww}^{-1/2} \mathbf{c}s(i) + \mathbf{w}'(i), \quad (23)$$

where $\mathbf{w}'(i) := \mathbf{R}_{ww}^{-1/2} \mathbf{w}(i)$ is white with identity covariance variance.

The MMSE estimator is: $\hat{s}(i) = \mathbf{g}_{mmse}^T \mathbf{y}(i) = \mathbf{c}^H \mathbf{R}_{ww}^{-1/2} \mathbf{y}'(i)$, which coincides with the maximal ratio combiner (MRC) output operating on (the pre-whitened) $\mathbf{y}'(i)$. Defining the equivalent code vector as $\mathbf{c}' := \mathbf{R}_{ww}^{-1/2} \mathbf{c}$, we reduce this colored problem to the white noise case studied in [13], and it is possible to obtain closed form expression (CFE) for the symbol error rate (SER).

First, we decompose the equivalent covariance matrix $\mathbf{R}_{c'c'} := \mathbb{E} \{ \mathbf{c}'(\mathbf{c}')^H \}$ as:

$$\mathbf{R}_{c'c'} := \mathbf{R}_{ww}^{-1/2} \mathbf{R}_{cc} \mathbf{R}_{ww}^{-1/2} = \mathbf{U}_{c'} \mathbf{D}_{c'} \mathbf{U}_{c'}^H, \quad (24)$$

where $\mathbf{U}_{c'}$ is $N \times (L+1)$ para-unitary and $\mathbf{D}_{c'}$ is a diagonal matrix with diagonal entries $\bar{\lambda}_{ii}, i = 1, 2, \dots, L+1$. The code covariance matrix \mathbf{R}_{cc} equals $\mathbb{E} \{ \mathbf{C} \mathbf{h} \mathbf{h}^H \mathbf{C}^H \}$.

As a result, a CFE can be obtained for the SER for MPSK (M constellation points) signals by direct substitution from [10, eq. (44)]:

$$P_s(E) = \frac{1}{\pi} \int_0^{(M-1)\pi/M} \prod_{i=1}^L I_i(\bar{\lambda}_{ii} \sigma_s^2 / \sigma_v^2, \gamma_{PSK}, \theta) d\theta, \quad (25)$$

where $\gamma_{PSK} := \sin^2(\pi/M)$, and $I_i(x, \gamma_{PSK}, \theta)$ is the moment of the probability density function of the equivalent channel h'_i evaluated at $-\gamma_{PSK} / \sin^2(\theta)$ (see [10, eq. (24)]); in our case $\sigma_v^2 \equiv 1$. The moment $I_i(x, \gamma_{PSK}, \theta)$ for distributions such as Rayleigh, Ricean, and the resulting SER for different constellations (e.g., QAM) may be found in [10].

Note that this procedure is applicable to any type of interference provided that the covariance matrix \mathbf{R}_{ww} (or, a consistent sample averaged estimate) is available.

Given the channel covariance matrix \mathbf{R}_{hh} , and the noise covariance matrix \mathbf{R}_{ww} , we can find the covariance matrix $\mathbf{R}_{c'} = \mathbf{R}_{ww}^{-1/2} \bar{\mathbf{C}}_{ds} \mathbf{R}_{hh} \bar{\mathbf{C}}_{ds}^H \mathbf{R}_{ww}^{-1/2}$ for DS-SS and $\mathbf{R}_{c'} = \mathbf{R}_{ww}^{-1/2} \mathbf{V} \mathbf{R}_{hh} \mathbf{V}^H \mathbf{R}_{ww}^{-1/2}$ for MC-SS. Having compared DS-SS with MC-SS under only NBI/PBI in Section 3, and only multipath in [13], we now test their performance in the joint presence of multipath and NBI/PBI via a simulation study.

We use the first channel model described in [13]; the channel \mathbf{h} is Gaussian distributed of order $L = 2$, i.i.d. with $\mathbf{R}_{hh} = \text{diag}(1, 1, 1)/3$; we use Gold codes of length 15. Now, narrow band interference is present in addition to multipath fading. We set the relative bandwidth of the NBI to $\epsilon = 3/16$, and the PSD ratio relative to the background noise as $10 \log_{10}(J_0/N_0) = 13\text{dB}$. Recall that if As1) holds, then the BER for MC-SS does not depend on code choices even in the presence of *both* multipath and NBI/PBI. Fig. 6 shows that the BER for MC-SS is lower than the average BER of DS-SS. Relative to the case without NBI/PBI, the gap between MC-SS and DS-SS increases when NBI/PBI is present as shown in Fig. 6, which corroborates the robustness of MC-SS (relative to DS-SS) with respect to frequency-selective multipath fading and narrow (or partial) band interference.

In this section, we compared MC-SS with DS-SS in the presence of both NBI/PBI and multipath fading. A closed-form expression for the SER was derived; it was seen that the BER for MC-SS is independent of the code in this case as well. We showed via simulations that MC-SS outperforms DS-SS in the case where degradations occur due to both multipath fading and NBI/PBI.

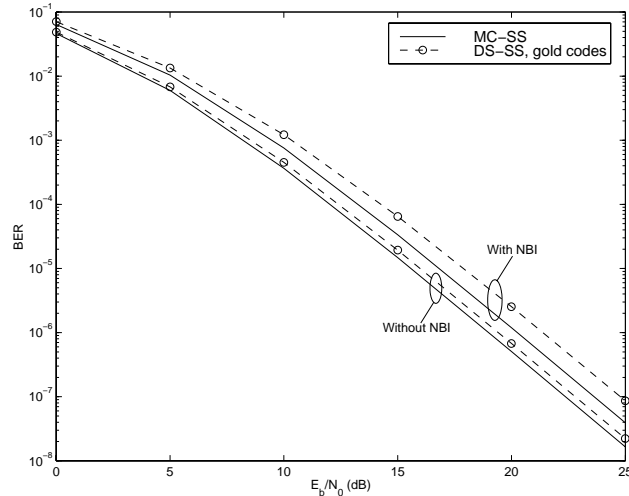


Figure 6. MC-SS vs DS-SS with NBI

5. CONCLUSIONS

We developed closed-form expressions for the BER performance of digital multi-carrier spread-spectrum (MC-SS) modulation; we then compared MC-SS with direct-sequence spread spectrum (DS-SS) under different scenarios: AWGN channel, NBI/PBI, and frequency-selective multipaths. The performance of MC-SS does not depend upon the spreading code; in contrast, the performance of DS-SS does depend upon the spreading code; to eliminate this code dependency one may hop between codes or use long codes. We showed that MC-SS with symbol periodic codes outperforms DS-SS with long codes or code hopping. The performance of DS-SS approaches that of MC-SS if the spreading gain is large and the codes are well chosen. In general, MC-SS outperforms DS-SS, particularly when both multipath fading and NBI/PBI are present.

REFERENCES

1. D. R. Brillinger, *Time Series: Data Analysis and Theory*, Holden-Day, Inc., expanded edition, 1981.
2. J. K. Cavers, "Optimized use of diversity modes in transmitter diversity systems," in *Proc. of the Vehicular Technology Conf.*, vol. **3**, pp. 1768–1773, 1999.
3. G. B. Giannakis, P. Anghel, and Z. Wang, "All-digital unification and equalization of generalized multi-carrier transmissions through frequency-selective uplink channels," *IEEE Transactions on Communications*, submitted Mar. 2000.
4. G. B. Giannakis and S. Zhou, "Optimal Transmit-Diversity Precoders for Random Fading Channels," in *Proc. of Globecom Conf.*, vol. **3**, pp. 1839–1843, San Francisco, CA, Nov. 27 - Dec. 1, 2000.
5. G. K. Kaleh, "Frequency-diversity spread-spectrum communication system to counter bandlimited Gaussian interference," *IEEE Transactions on Communications*, vol. **44**, no. 7, pp. 886–893, July 1996.
6. S. Kondo and L. B. Milstein, "Performance of multicarrier DS CDMA systems," *IEEE Transactions on Communications*, vol. **44**, no. 2, pp. 238–46, Feb. 1996.
7. S. Parkvall, "Variability of user performance in cellular DS-CDMA—long versus short spreading sequences," *IEEE Transactions on Communications*, vol. **48**, no. 7, pp. 1178–1187, July 2000.
8. J. Proakis, *Digital Communications*, McGraw-Hill, 1996.
9. G. J. Saulnier, M. Mettke, and M. J. Medley, "Performance of an OFDM spread spectrum communication system using lapped transforms," in *Military Communications Conference*, vol.2, pp. 608 -612, 1997.
10. M. K. Simon and M.-S. Alouini, "A unified approach to the performance analysis of digital communication over generalized fading channels," *Proceedings of the IEEE*, vol. **86**, no. 9, pp. 1860–1877, Sept. 1998.
11. Z. Wang and G. B. Giannakis, "Wireless multicarrier communications: Where Fourier meets Shannon," *IEEE Signal Processing Magazine*, pp. 29–48, May 2000.
12. N. Yee, J-P. Linnartz, and G. Fettweis, "Multicarrier CDMA in indoor wireless radio networks," in *Proc. IEEE PIMRC*, 109–113, Sept. 1993.
13. S. Zhou, G. B. Giannakis and A. Swami, "Comparison of digital multi-carrier spread spectrum and direct sequence spread spectrum in the presence of multipath", in *Proc. ICASSP'01*, Salt Lake City, May 7-11, 2001.